Weight reduction of DC/DC converters using controllable inductors

Dennis Eichhorst, Jonas Pfeiffer, Peter Zacharias

University of Kassel, Germany

Corresponding author: Dennis Eichhorst, dennis.eichhorst@freenet.de

Abstract

Controllable inductors can be realized by introducing auxiliary windings into the device that partially saturate the core and allow variation of the inductance value. This can be used to achieve zero-voltage switching in a DC/DC converter over a wide load range while at the same time the weight of the inductor is reduced. In this paper the possible size and weight reduction and the influence on the efficiency is calculated and compared to other solutions. The results are verified in a prototype.

Acknowledgements

Parts of the work presented in this paper have been supported by the BMBF (German Federal Ministry of Education and Research). Project funding reference number: 16EMO0234. Responsibility for the contents of this publication lies with the authors.

1 Introduction

Magnetic devices are among the components with the largest influence on the total weight in most power electronic converters. These heavy components not only increase the weight and size by itself, but also by support structures that are needed to fix them into position. This is particularly relevant in any mobile use such as automotive, railway or portable applications, where the weight must be lifted or accelerated.

Increasing the switching frequency of the power converter is one important solution to reduce the size of the inductive components. Recently, wide-band-gap semiconductors played an important role to the increase of the switching frequency. Due to the currently higher costs of the wide-band-gap devices and technical challenges in the effective use of them, silicon-based switches still have a much larger share in the power semiconductor market.

Soft-switching is another approach to increase the switching frequency or reduce power losses in the converter. Soft-switching topologies using resonances between one or more capacitors and inductors in the power circuit or in parallel to the semiconductor are available for most power conversion applications. Typically, they need additional components or have a limited power or voltage range in which resonant switching is possible.

In this paper a full-bridge DC/DC converter which is operated in the triangular current mode (TCM) will be investigated. This operation mode is known e.g. from [1], [2]. Using TCM, the semiconductor switches are turned on when the current through them will be slightly negative, therefore allowing quasi zero-voltage-switching (ZVS) and especially omitting recovery losses of the antiparallel diode. To achieve this mode of operation over a wide output current range a controllable inductor is used to vary the steepness of the current slope in the semiconductors. This allows for an increased efficiency compared to an operation with variable or even constant switching frequency.

ISBN 978-3-8007-4938-6

2 Controllable inductors

Controllable magnetic devices can be realized by introducing a (in the sense main winding) parallel or orthogonal magnetic flux in the magnetic core, which saturates the core material or parts of it [3]. It can be realized with an auxiliary winding which is either parallel to the main flux (the winding leads vertically through the limb of the core) or orthogonal to it (the winding leads through the yoke). The auxiliary winding only influences the main current waveform by changing the inductance of the choke.

The first solution applies a pot core which center hole is used for the integration of the auxiliary winding as can be seen in Fig. 1. It is therefore parallel to the main flux. A direct current signal in the auxiliary winding causes an increased flux density depending on the distance from this winding, with the flux density highest next to it. Increasing the current saturates the core from the inside to the outside, reducing the inductance of the magnetic device. The second solution is the so-called virtual air-gap (VAG) concept, which is described in detail in [4]. It allows the saturation of a defined, small part of the core by having two antiparallel windings. These windings are integrated into the core through 4 holes in the yoke (Fig. 2). This leads to a very high flux density near the auxiliary windings, while in distance the magnetic flux of them cancel each other out. The saturated part behaves like an air-gap with variable size depending on the auxiliary current.

The first solution can be implemented easily when using a pot core with a mounting hole, while the

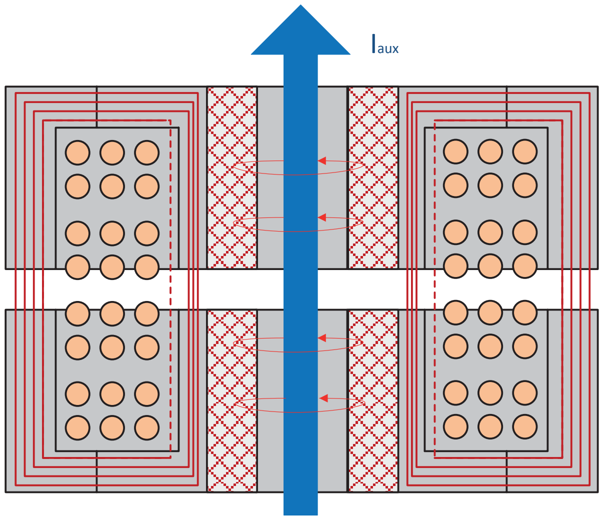

Fig. 1: Cross section of a choke based on a pot core with parallel auxiliary current (blue)

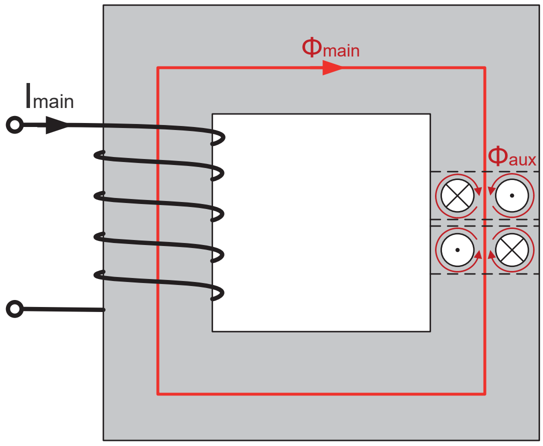

Fig. 2: Choke with auxiliary winding orthogonal to the main flux

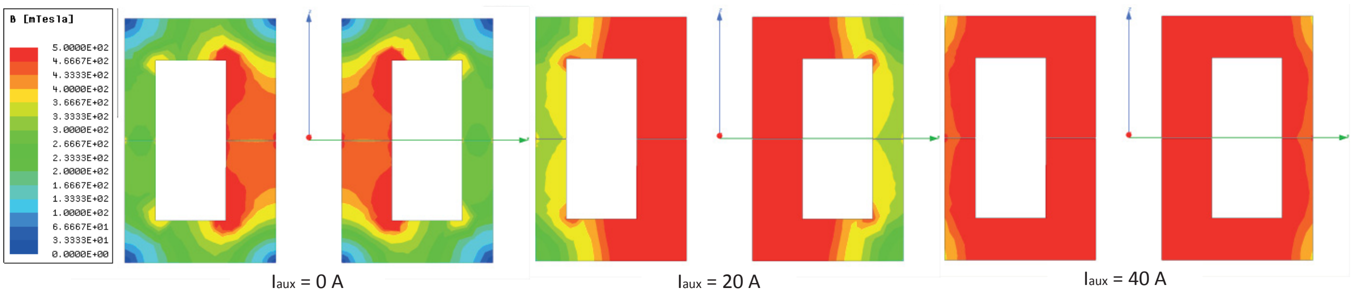

Fig. 3: Influence on pre-magnetization with a parallel winding on the flux density (pot-core)

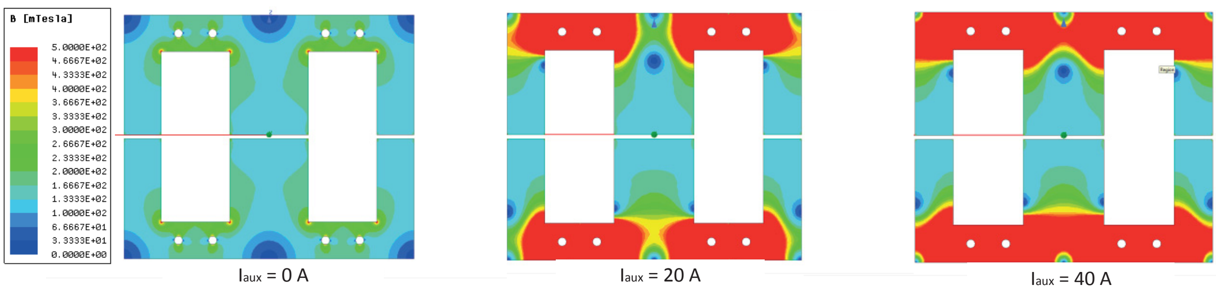

Fig. 4: Influence of the pre-magnetization with an orthogonal winding (virtual air-gap) on the flux density

additional holes of the second solution require a modification of existing core types. On the other hand, the second solution seems more promising to vary the inductance value over a wide range.

The magnetic flux density in the magnetic core in vicinity of the auxiliary windings have been simulated using ANSYS Maxwell for both a parallel and orthogonal auxiliary winding (i.e. using a P30/19 pot core and an E34/14/9 E-core). The results can be seen in Fig. 3 and Fig. 4.

3 Using controllable inductors to achieve TCM operation

As mentioned, switching a semiconductor into ON-state when the current in that instant is negative will largely reduce the switching losses. Considering the full-bridge converter (Fig. 5), the switching pattern of the transistors is realized as shown in Fig. 6. The low-side switches are operated complementary to their high-side devices. This pattern is referred to as unipolar voltage switching in e.g. [5]. A dead-time between the switching operation of the transistors in a half-bridge is introduced to avoid cross-conduction.

When the current through the high-side switch is negative in the instant of turn-on, the current will already start to flow through the antiparallel diode of the switch (in case of a MOSFET its body-diode) during the dead-time. Therefore, in the actual switching instant, the voltage present at the half-bridge drops mainly at the low-side switch and the high-side switch turns on under ZVS condition.

Additional losses usually occur when the body-diode of the low-side transistor is turned-off (because of the high-switch becoming active). Its recovery charge will then flow through the high-side transistor, which is just in the process of turning on, carrying this additional current when the voltage at the device has not dropped to zero. When the low side MOSFET is turned-off carrying an already positive current, its body-diode will not

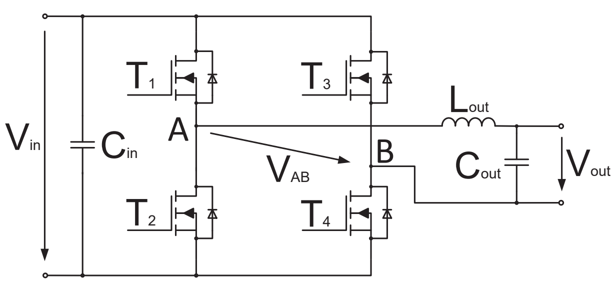

Fig. 5: Schematic of the full bridge converter

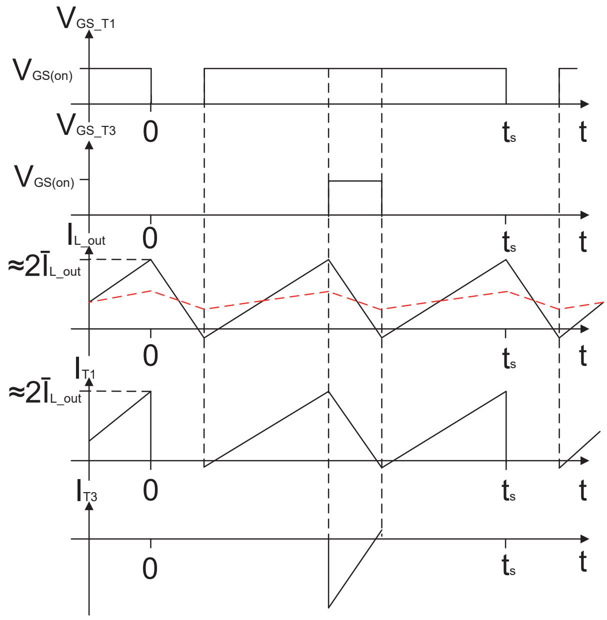

Fig. 6: Control signals, output choke current, and current trough the semiconductors for TCM operation (CCM choke current indicated in red for comparison)

become conductive during the dead-time and the recovery losses are avoided.

Using backward conduction in a bridge circuit is referred to as synchronous current mode (SCM) in the literature (e.g. [6]). In SCM the amplitude of the choke current remains constant, while only its average current changes depending on the output load. This leads to a relatively high rms current in the choke and in the semiconductors at low load operation, which results in a low efficiency at light load conditions. Generally, the rms current in the power electronic devices of the circuit is higher due to the triangular current shape, compared to the nearly rectangular shape typical in designs that lack the possibility of ZVS. The reduced switching losses are therefore often associated with increased conduction losses.

The amplitude of the current is determined by the input and output voltage V_{in}, V_{out}, the output inductance L_{out} and the on-time of the semiconductor T2 according to the formula

$$\Delta I = \frac{V_{in} - V_{out}}{L_{out}} t_{T2on} \quad (1)$$

While the input and output voltage and therefore the necessary duty-cycle are design requirements and cannot be changed, one possibility is to reduce the on-time by increasing the switching frequency depending on the output current, which is a typical realization of TCM. The target is to set the output frequency in a way that the current amplitude in the output choke is only slightly larger than double its average current, resulting in a short time of negative current only at the instant of switching the semiconductors. In this way the rms-value of the current is minimized. On the other hand, the increased switching frequency results in additional switching losses at low load.

As Eq. (1) shows, the amplitude of the choke current also depends on the output inductance. The controllable inductors introduced in chapter 2 allow for the reduction of its nominal inductance up to a factor of 10, which makes them suitable to achieve TCM operation down to 10% of the nominal output current of the converter. At the same time, the magnetic flux density remains constant in that range, allowing for an optimal utilization of the magnetic core. Additionally, due the higher inductance available at low output current, the output voltage ripple will be lower under this operating condition.

4 Design and simulation of the converter

A 300 W 48V/12V full-bridge converter has been designed. While this is not the typical topology for non-isolated DC/DC conversion, it allows for investigating step-up as well as step-down operation and even alternating current applications are possible with the same principle as described in chapter 3.

For the semiconductor switches Infineon IPP039N10N05 Si-MOSFETs were used, which resulted in lowest total losses at full load compared to types with deviating on-state resistance. For the fixed frequency operation 50 kHz was chosen, this is also the minimum value for variable frequency converter.

The output chokes apply N87 material of TDK/Epcos except for the converter with variable frequency, which is calculated without core for weight reduction. The core losses were calculated using the improved generalized Steinmetz equation [7] and compensating for current bias as shown in [8]. The winding is implemented using 180 x 0.2 mm litz-wire to decrease skin-effect losses, which can be especially high in the TCM converter. Proximity losses have not been calculated because that would have required sophisticated 3-D FEM models to determine the influence of the variable saturation. The results of the choke design are shown in Tab. 1.

A comparison of the power loss distribution is shown in Fig. 7. Losses in filter capacitors, control electronics, auxiliary winding and further conduction losses in the circuit have also been considered therein. As expected, the conduction losses are higher in the converters operated in TCM, while the switching losses are comparable. The recovery-losses caused by the body-diode in CCM operation are low, eliminating them in the TCM is obviously not enough to achieve a higher efficiency of the converter. Moreover, core losses in the controllable inductance are higher, which is lower the efficiency especially at low load. In total, the efficiency of the converter with variable inductance is about 0.5 % less than in the conventional design. The converter applying a variable switching frequency to achieve TCM operation on the other hand shows high switching losses and conduction losses (caused by the body-diode) in the low load region. This results in a very bad efficiency at that point of operation while at

Tab. 1: Comparison of output choke designs for 48V/12V converter

	Conventional	Variable frequency	Parallel aux. winding	Orthogonal aux. winding
Inductance	11.2 µH	1.12 µH	1.75 – 17.5 µH	1.75 – 17.5 µH
Core	P41/25	Air – 10 mm diam.	P30/19	E34/14/9
Turns	6	14	3	5
Total weight	102.2 g	24 g	45.7 g	46.6 g
Total losses	1.69 W	0.68 W	1.91 W	1.96 W
Req. output capacitance	31µF	310 µF	173 µF	173 µF

ISBN 978-3-8007-4938-6

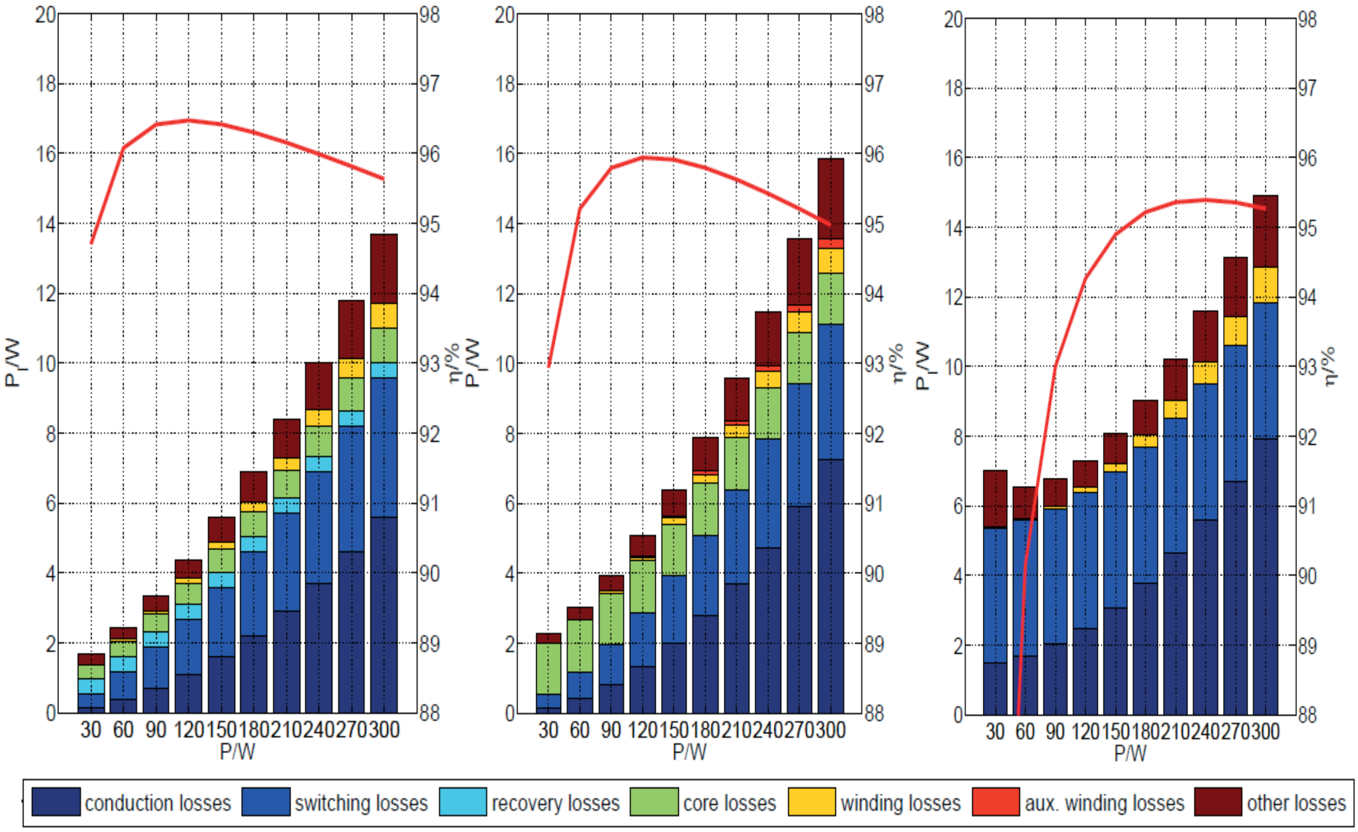

Fig. 7: Calculated power loss distribution and efficiency for 48V/12V converter. Left: conventional inductor, middle: controllable inductor, right: variable switching frequency

nominal load, the efficiency is even slightly higher as calculated with the variable inductance.

A direct voltage control for the converter with variable inductance has been designed. This can be done using the same design principles as for a fixed inductance values if for the corner frequency of the output filter the maximum value of L_{out} is considered. The converter has been simulated using PLECS to verify the aforementioned efficiency calculation and to further investigate the dynamic behavior. Both the conventional converter and the one with variable inductance showed similar step-response behavior, demonstrating that no additional effort is necessary to control the output voltage. Nonetheless, a control of the output inductance is required to maintain ZVS when the output current changes. Given the fact that the inductance value depends nonlinearly of the control voltage, especially because of the hysteresis of the core material, either a sophisticated control method or an acceptable approximation realizing ZVS over a wide load range must be found. This important issue is still under investigation.

The weight reduction resulting from the use of the controllable inductor is a good achievement. But improvements in the efficiency could not be realized due to the low recovery losses in this low voltage application. Avoiding them is not sufficient to outweigh the increased conduction losses in the semiconductors.

Therefore, further investigations were made with a converter having an input voltage of 400 V and an output voltage of 100 V at the same output power level. This converter applies SiC-MOSFETs SCT3030AL from Rohm. The output chokes have been modified to achieve a comparable output behavior to the low voltage converter using the same magnetic core elements. The main parameters of this chokes can be seen in Tab. 2.

While recovery charges of the body-diode in SiC semiconductor and the Si low voltage device used in the first design are comparable, the increased input voltage leads to a tenfold increase of the recovery losses. At the same time, the conduction losses are much lower in this application because of the reduced output current while at the same time the $R_{DS(on)}$ of the MOSFET is increased by a factor of 10. In total, this leads to superior efficiency of the TCM converter over the whole load range, being 1.5 % higher at nominal load and nearly 7 % at 20 % of the nominal load (Fig. 8).

ISBN 978-3-8007-4938-6

Tab. 2: Comparison of output choke designs for the 400V/100V converter

	Conventional	Parallel aux. winding
Inductance	0.92 mH	0.12 – 1.2 mH
Core	P41/25	P30/19
Turns	42	27
Total weight	105 g	45.2 g
Total losses	1.69 W	1.79 W
Req. output capacitance	300 nF	2,5 µF

5 Verification and conclusion

A prototype has been built to demonstrate the operating principle of a converter with variable inductance and to verify the calculated efficiency of the converter. Firstly, it was investigated whether the controllable magnetics can be used to modify the choke current as desired. It showed that the inductance of the choke with parallel auxiliary winding could only be reduced to about 50 % of its nominal value while the orthogonal auxiliary winding allowed for less than 20%. At the same time only half of the control current is needed (which also means that the losses in the control winding are 75 % less). The choke applying the virtual air-gap is therefore more adequate for the use as a controllable inductance. One additional challenge was the exact realization of the required inductance value with the very small air-gap necessary. While increasing the number of turns and the air-gap could be a possible solution, this also decreases the controllable range of the inductor because the increased air-gap length adds up to the virtual air-gap generated by the auxiliary winding. To achieve a useful design for

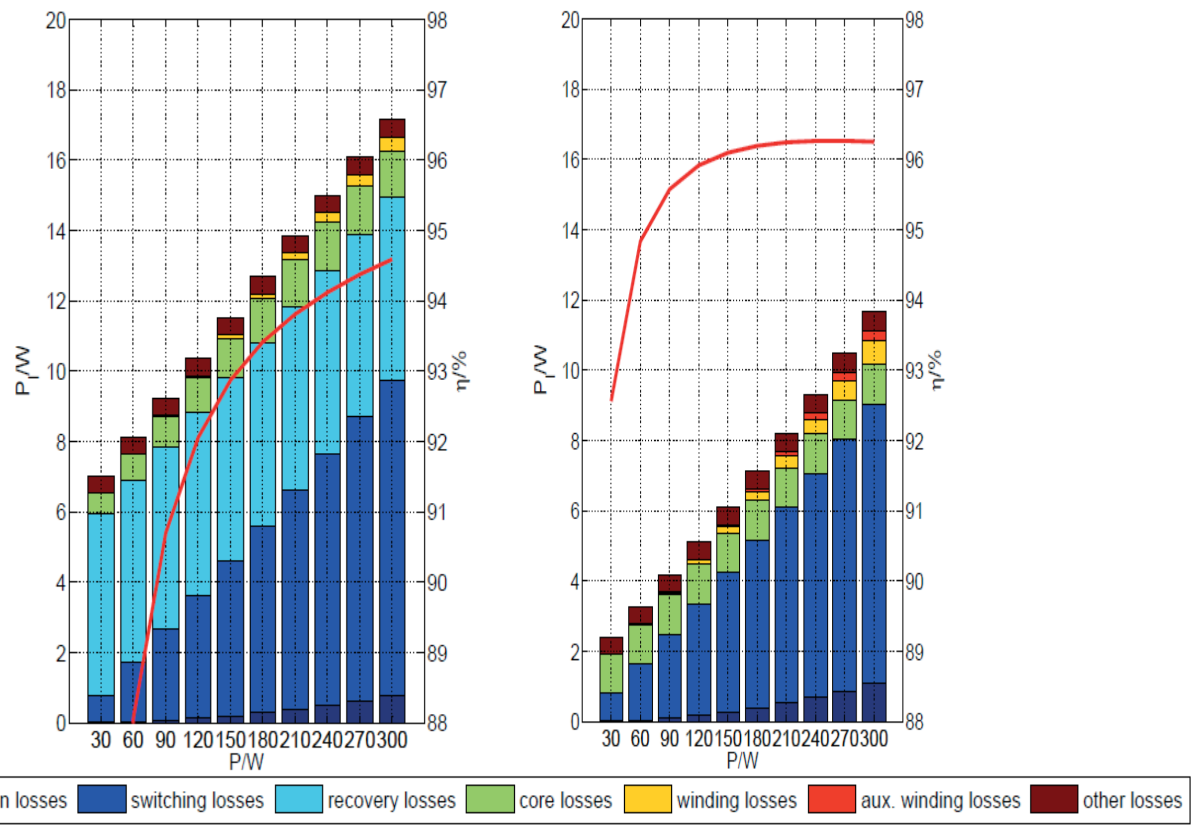

Fig. 8: Calculated power loss distribution and efficiency for 400V/100V converter. Left: conventional inductor, right: controllable inductor

ISBN 978-3-8007-4938-6

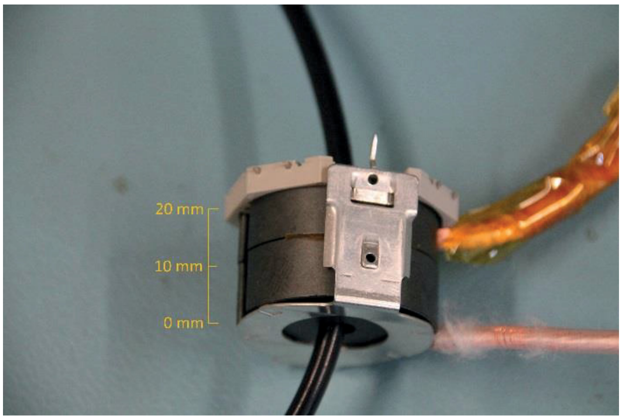

Fig. 9: Output choke with auxiliary winding in parallel to the main flux

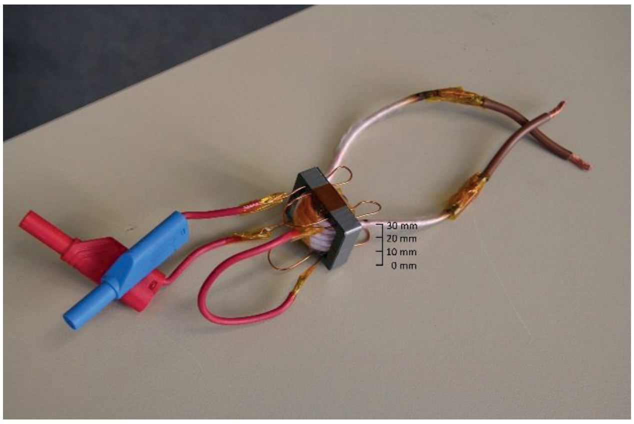

Fig. 10: Output choke with auxiliary winding orthogonal to the main flux

the E-core choke, the parameters have been changed in the functional sample to 4 turns and an air-gap length of approx. 1 mm.

The efficiency measured for the 48V/12V was always less than calculated in the section above. This deviation is caused by increased conduction losses in the circuit. Due to non-ideal test setup the resistance of the current path and the influence of skin-effect could not always be minimized. Moreover, oscillation between source and output filter of the converter lead to an additional share of apparent current in the circuit, further increasing the conduction losses.

The increased resistance is especially critical in case of the TCM operation, because of the anyway higher rms-current in most parts of the circuit. The efficiency at high load is more than 2 % less than for the conventional converter. At low load, results equal the calculation, except for the converter with the choke applying a parallel auxiliary winding. Here, the inductance value could only be variated

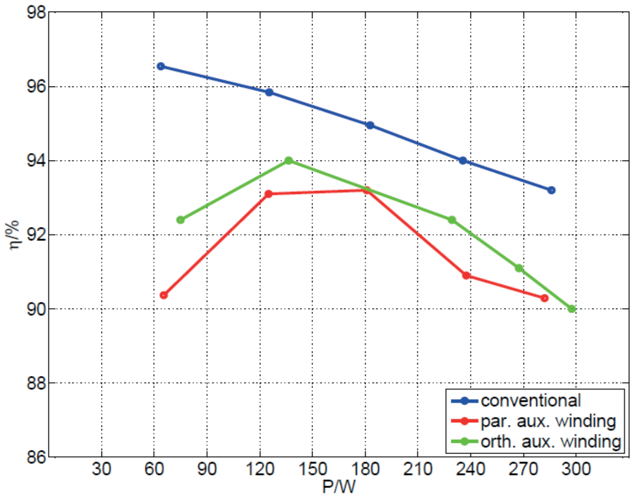

Fig. 11: Comparison of efficiency for different output chokes (calculated P_{out}/P_{in}), 48V/12V converter

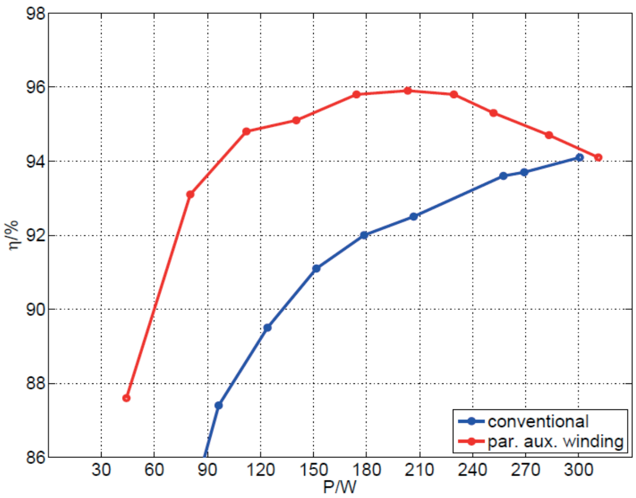

Fig. 12: Comparison of efficiency for different output chokes (calculated P_{out}/P_{in}), 400V/100V converter

between 50 % and 100 % of the output power, hence the conduction losses are high at low load (Fig. 11).

The 300 W 400V/100V converter prototype basically suffers from the same limitations, but the influence is far less because of the low operation current. Consequently, the measurement results shown in Fig. 12 deviate less from the calculated values. The efficiency of the converter with controllable output choke is higher than the conventional one over the whole load range. Deviations to the calculations for the TCM operations are caused by a very high control current at maximum load which increased the auxiliary winding losses. Furthermore, no

ISBN 978-3-8007-4938-6

inductance control was possible below 150 W, which increased conduction and switching losses in that range.

In this paper it has been demonstrated that the triangular current mode in a DC/DC converter could not only be achieved by means of a variable switching frequency, but also by a variable inductance. The advantages of the variable inductance are reduced switching losses at low inductance current and therefore increased efficiency at light load. Both designs realize output chokes weighing 55 – 75 % less than the conventional design for CCM. The influence of the larger output capacitor is negligible, the additional weight is only ca. 0.3 g. While the coreless choke for the variable frequency operation is the most lightweight solution, the lack of an iron core might likely worsen the EMC behavior of the converter.

The use of the variable inductance proved especially promising at high voltage applications with comparably low conduction losses. An increased efficiency could then be realized even when SiC semiconductors are applied. This might make other countermeasures to recovery losses like additional antiparallel SiC schottky diodes obsolete.

Additional effort is needed realize the control and supply of the control current. During the measurements, a current up to 100 A was necessary (using only one turn) but increasing the number of turns or introduce more auxiliary windings at different positions of the core can minimize the requirements of the source. Another solution can be feeding the output current through the auxiliary winding to realize most of the auxiliary flux while the precise setting is done by a second parallel winding consequently needs a smaller source than if it would have to carry the whole auxiliary current.

6 References:

[1] C. Marxgut, J. Biela and J. W. Kolar: Interleaved triangular current mode (TCM) resonant transition, single phase PFC rectifier with high efficiency and high power density. *Proc. Int. Power Electron. Conf.*, 2010, pp. 1725–1732.

[2] O. Knecht, D. Bortis and J. W. Kolar: Comparative Evaluation of a Triangular Current Mode (TCM) and Clamp-Switch TCM DC-DC Boost Converter- Energy Conversion Congress and Exposition (ECCE), 2016 IEEE. :1-8 Sep, 2016

[3] P. Zacharias, T. Kleeb, F. Fenske, J. Wende, J. Pfeiffer: Controlled Magnetic Devices in Power Electronic Applications. 19th European Conference on Power Electronics and Applications, EPE'17 ECCE,2017

[4] D. Dolan. and P. Lehn: Analysis of a Virtual Air Gap Variable Reactor. IEEE Power Electronic Specialists Conference (PESC), 2007

[5] N. Mohan, T. Undeland, W. Robbins: Power Electronics - Converters, Applications and Design. 3rd Edition., Hoboken: John Wiley and Sons, Inc, 2003

[6] J. S. Lai, B. York, A. Koran, Y. Cho, B. Whitaker, and H. Miwa: High-efficiency design of multiphase synchronous mode soft-switching converter for wide input and load range. Proc. Int. Power Electron. Conf. (IPEC), 2010, pp. 1849–1855.

[7] K. Venkatachalam, C. R. Sullivan, T. Abdallah, and H. Tacca: Accurate Prediction of Ferrite Core Loss with Nonsinusoidal Waveforms Using only Steinmetz Parameters. Proc. IEEE Workshop Comput. Power Electron., 2002, S. 36 - 41.

[8] J. Mühletaler, J. Biela, W. Kolar, A. Ecklebe: Core Losses under the DC Bias Condition Based on Steinmetz Parameters. IEEE Transactions on Power Electronics, Vol. 27, No. 2, Feb. 2012, S. 953 - 962

ISBN 978-3-8007-4938-6